

Proceedings of the ASME 2020 International Technical Conference and Exhibition on Packaging and Integration of Electronic and Photonic Microsystems
InterPACK2020
October 27-29, 2020, Virtual, Online

IPACK2020-2590

CFD MODELING OF THE DISTRIBUTION OF AIRBORNE PARTICULATE CONTAMINANTS INSIDE DATA CENTER HARDWARE

Satyam Saini¹, Kaustubh K. Adsul, Pardeep Shahi, Amirreza Niazmand, Pratik Bansode, Dereje Agonafer

The University of Texas at Arlington Arlington, TX

ABSTRACT

Modern-day data center administrators are finding it increasingly difficult to lower the costs incurred in mechanical cooling of their IT equipment. This is especially true for high-performance computing facilities like Artificial Intelligence, Bitcoin Mining, and Deep Learning, etc. Airside Economization or free air cooling has been out there as a technology for a long time now to reduce the mechanical cooling costs. In free air cooling, under favorable ambient conditions of temperature and humidity, outside air can be used for cooling the IT equipment. In doing so, the IT equipment is exposed to sub-micron particulate/gaseous contaminants that might enter the data center facility with the cooling airflow.

The present investigation uses a computational approach to model the airflow paths of particulate contaminants entering inside the IT equipment using a commercially available CFD code. A Discrete Phase Particle modeling approach is chosen to calculate trajectories of the dispersed contaminants. Standard RANS approach is used to model the airflow in the airflow and the particles are superimposed on the flow field by the CFD solver using Lagrangian particle tracking. The server geometry was modeled in 2-D with a combination of rectangular and cylindrical obstructions. This was done to comprehend the effect of change in the obstruction type and aspect ratio on particle distribution. Identifying such discrete areas of contaminant proliferation based on concentration fields due to changing geometries will help with the mitigation of particulate contamination related failures in data centers.

Keywords: CFD, particle transport, data center, contamination.

NOMENCI ATURE

MOMITME	AIUNL
ACH	Air Change per Hour
CFD	Computational Fluid Dynamics
CBB	Confined Bluff Body
DPM	Diesel Particulate Matter
DRH	Deliquescent Relative Humidity
ISO	International Standards Organization
MERV	Minimum Efficiency Reporting Value
PCB	Printed Circuit Board
RANS	Reynolds Averaged Navier Stokes
_	- 11 - 1

Re Reynolds Number

SIMPLE Semi Implicit Method for Pressure Linked

Equations

SIR Surface Insulation Resistance

INTRODUCTION

With a significant increase in computational demand over the last decade due to developments in AI (Artificial Intelligence) and machine learning, bitcoin mining, cloud computing, etc., data center proliferation has skyrocketed. While novel cooling techniques like dielectric fluid immersion cooling and indirect liquid cooling are being used to dissipate significantly high heat fluxes, air cooling still dominates the data center cooling industry and it will continue to do so. Since the HVAC systems are accountable for a major part of energy consumption in typical air-cooled data centers, it becomes imperative to improve the efficiency of the cooling systems. One of the many causes of inefficiencies in an air-cooled data center

¹ Contact author: satyam.saini@mavs.uta.edu

is the power consumption of cooling hardware like CRACs and chilled water systems.

Conventional data centers that are located in cold geographies, operate year-round using mechanical cooling without taking the advantage of seasonal or local climatic conditions to cool the IT equipment. Airside economization accomplishes this by bringing outside air at low ambient temperature and relative humidity to reduce the work done by mechanical compressors in the CRAC units for a major part of the year, thus, saving energy expenditure. The ASHRAE T.C.9.9 subcommittee on Mission Critical Facilities, Data Centers, Technology Spaces and Electronic equipment defines temperature and humidity range guidelines to ensure reliable operation of IT equipment [1-6]. They are accepted by ITE manufacturers and their clients to be as follows: 18°C to 27°C (64.4°F to 80.6°F) dry bulb temperature, -9°C to 15°C (41.9°F) to 59°F) dew point temperature, and less than 60% relative humidity. The recommended envelope was expanded by ASHRAE Thermal Guidelines for Data Processing Environments 2008, thereby, allowing short excursions into the allowable regions A1-A3, as shown in Figure 1, and an increase in the number of economizer hours.

	Equipment Environmental Specifications for Air Cooling						
		Produc	t Operations ^{b,c}		Product Power Off ^{c,d}		
Class ^a Dry-Bulb Temperature ^a	Temperature*4	Humidity Range, Non-Condensing ^{h,l,k,l}	Maximum Dew Point ^a *C	Maximum Elevation ^{e,j,m} m	Maximum Temperature Change' in an Hour (°C)	Dry-Bulb Temperature °C	Relative Humidity ^h %
		Recomi	mended (Suital	ble for all 4 cla	sses)		
A1 to	18 to 27	-9°C DP to 15°C					
A4	18 to 27	DP and 60% RH					
Allowab	le						
A1	15 to 32	-12°C DP & 8% RH to 17°C DP and 80% RH ^k	17	3050	5/20	5 to 45	8 to 80
A2	10 to 35	-12°C DP & 8% RH to 21°C DP and 80% RH ^k	21	3050	5/20	5 to 45	8 to 80
А3	5 to 40	-12°C DP & 8% RH to 24°C DP and 85% RH ^k	24	3050	5/20	5 to 45	8 to 80
A4	5 to 45	-12°C DP & 8% RH to 24°C DP and 90% RH ^k	24	3050	5/20	5 to 45	8 to 80
В	5 to 35	8% to 28*C DP and 80% RH ^k	28	3050	NA	5 to 45	8 to 80
С	5 to 40	8% to 28°C DP and 80% RH ^k	28	3050	NA	5 to 45	8 to 80

FIGURE 1: ASHRAE 2015 TEMPERATURE GUIDELINES SHOWING THE RECOMMENDED AND ALLOWABLE RANGES FOR TEMPERATURE AND HUMIDITY FOR DATA CENTERS [6]

While companies like Microsoft and Facebook have been able to achieve PUE values as low as 1.1 using free air-cooling methods in geographies with favorable climatic conditions throughout the year, many data center administrators are still reluctant to implement airside economization [6-9]. This is owed to the inherent risk of bringing in particulate and gaseous contaminants along with the outside air. Improvement in computational performance is achieved with a reduction in transistor channel lengths, thus, increasing packaging densities. The net impact of this scaling down results in a subsequent increase in the probability of contamination related failures as higher packaging densities require higher velocities for cooling. Literature suggests that higher velocities increase the particle accumulation rate as well, thus making the closely packed

features on PCBs more susceptible to failures related to settled hygroscopic matter [reference on accumulation]. Under the influence of particulate and gaseous contaminants, electronic components and PCBs fail in two ways: Electrical open circuits caused due to corrosion, for example, of silver terminations in surface mount resistors due to the presence of sulfur-bearing gases [10-14]; Electrical short-circuits due to copper creep corrosion, ECM (Electro Chemical Migration), and cathodicanodic filamentation [12]. These failure modes led to new industry-accepted specifications for contamination limits, which now place a lower limit on the DRH of dust [15, 16]. Also, research by ASHRAE Technical Committee (TC) 9.9 for Mission Critical Facilities, Technology Spaces, and Electronic Equipment led to the publication of a white paper [21] and a book among the Datcom Series [17] on contamination guidelines for data centers and the formulation of new gaseous contamination limits used to update ISA Standard 71.04-2013 [18]. This research also led to the publication of an iNEMI position paper [19] on gaseous contamination as well as current efforts to update the Chinese data center design guide GB 50174-2008 [20] to include gaseous contamination limits.

The challenging part of simulating particle flow inside the servers is the presence of a multitude of bluff bodies of varying geometries that produce eddies that produce numerous adverse pressure gradients around these objects. This study is an extension of the authors' previously published work where a simplified model of a raised floor data center space was developed to visualize particle transport at room level [21]. A similar approach was used where a transient CFD analysis was done for simplified 2-D models of the servers with large obstructions like heat sinks, DIMMs were created for different server configurations. The flow and particle transport models were studied from existing literature, as presented below, on particle transport in ducts and 2-D channels with/without obstructions. This enabled the authors to significantly simplify the problem and formulate a set of assumptions that closely matched the flow characteristics inside a real server. The particle dispersion results were reported by analyzing the time spent by a specified particle mass flow rate in the flow domain, the particle mass entering and leaving the domain at steady state, and average instantaneous particle volume fraction in the domain.

LITERATURE REVIEW

The issue of data center contamination due to settled particulate matter has been mostly discussed in the form of case studies, from a risk assessment point of view, and mostly addresses the best practices to mitigate harmful contaminants [22,23]. The current literature is dominated by empirical studies that have investigated the failure modes and failure mechanisms, dominated by corrosion studies at PCB level and interconnect level. Particle laden flow, in general, has been studied widely for commercial buildings and indoor residential environments owing to high risk to the occupants [24-26]. An in-depth literature review was done for particle dispersion and deposition studies in ducts and across bluff bodies of various geometries. Several experimental [27,28] and numerical [29-32,53]

investigations have studied the phenomena of particle dispersion in shear flows, where the flow regime is dominated by large vortex formations [33]. More recent work on particle-laden channel flow with Confined Bluff Bodies (CBB) flow can be found in, for example, Breuer and Alletto [34], Mallouppas and vanWachem [35], Sardina, Schlatter, Brandt, Picano, and Casciola [36] and Wang, Manhart, and Zhang [37], while turbulence modification in turbulent particle-laden channel flows can be found in Vreman [38, 39]. A review study was done by experts at LBNL on experimental and theoretical work deposition of particulate matter in turbulent flow in HVAC ducts [40].

The deposition efficiency of liquid particles in 5.03–8.51 mm diameter circular cross-section tubes was investigated by Pui et al. for both turbulent and laminar flows [41]. Particle transport and deposition in vertical and horizontal turbulent square duct flows were studied by Zhang and Ahmadi for different gravity directions [42]. This study implemented the Direct Numerical Simulation of the Navier-Stokes equation to provide that particle deposition velocity varies as per the direction of gravity. It was concluded that for horizontal ducts, because of gravity, particle deposition velocity on all four surfaces of the square duct is distinct. Most of the previous works have investigated particle sizes of less than 10µm. However, a study carried out by Zhao and Wu brought something new to the particle size selection [43]. Particle size distribution deposited on the ventilation duct was investigated in a room (4 m x 2.5 m x 3 m) with a typical mechanical ventilation system. The air supply volume rate was 240m³/hour and the corresponding air change rate was 8 air changes per hour (ACH). The study reported that although the particle diameters smaller than 10 µm are the majorly airborne through the duct, the particles deposited on the duct surface are mostly larger than 10 µm [44]. Frankenthal et al developed a submicron particle exposure chamber for life testing of circuit boards due to ionic particle exposure [45]. This study also cites some archival literature that makes predictions on particle accumulation rates based on particle sizes and types as shown in Table 2 and Table 3. As can be seen from the data below, the deposition velocities are highly dependent on airflow velocity and particle size.

	Adolscent pollutants (0.01-01 µm)	Mature Pollutants (0.1-1 μm)	Mineral Biologicals (1-15 μm)
Outdoor	0.6-6	0.6	0.6
Office	0.009-0.6	0.006	0.6
building			
Class 10	0.06-0.9	0.009-0.09	0.6
Cleanroom			

TABLE 1: DEPOSITION VELOCITIES FOR AIRBORNE PARTICLES (CM/S) [45]

	Adolscent pollutants	Mature Pollutants	Mineral Biologicals
	(0.01-01 µm)	(0.1-1 μm)	(1-15 μm)
0-41	$2 \times 10^7 - 2 \times$	2 x 10 ⁴ - 2 x	$2 \times 10^2 - 2 \times$
Outdoor		_	
	10^{10}	10^{7}	10^{4}
Office	30 - 2 x 10 ⁶	$2 \times 10^3 - 2 \times$	2 - 200
building		10^{4}	
Class 10	0.2-150	0.003 - 0.3	0.001 - 0.2
Cleanroom			

TABLE 2: ACCUMULATION RATES FOR AIRBORNE PARTICLES (PARTICLES/M²S) [45]

NUMERICAL METHOD

Particle-laden flow is a common phenomenon for many practical daily indoor and technical applications. CFD enables detailed prediction of complex fluid flows by discretizing complex geometries into smaller regions and numerically solving the desired flow characteristics in these individual discretized regions. Commercially available CFD codes have made it easier to visualize complicated flow phenomena like particle-particle interactions and particle-flow interactions. Lagrange-Euler approach has been proven to solve multiphase particle-laden flows. This approach uses RANS equations to solve the continuous or carrier phase and the dispersed or particle phase is resolved by Lagrangian tracking. The CFD code was chosen based on its extensive abilities in resolving particleparticle, particle-flow interactions, and accurate mathematical models in simulating turbulence involved in particle flow. As described in ANSYS FLUENT Theory guide [46,47], the continuous phase is calculated using the RANS equations as given below:

$$\nabla . \, \bar{u} = 0 \tag{1}$$

$$\frac{\partial u}{\partial t} + \rho \ (\bar{u}.\nabla)\bar{u} = -\nabla \bar{p} + \eta \Delta \bar{u} - \nabla.\overline{\tau^{RS}} + \bar{f}_D \tag{2}$$

Where \bar{u} and \bar{p} are the average velocities of continuous (air) and discrete (particle) phase. The second term on the left-hand side in equation (2) represents the Reynolds Stresses which are modeled using the eddy-viscosity approach. In this study, the standard κ - ω model was used to model kinetic energy and turbulent dissipation. Equations (3), (4) and, (5) are solved to obtain the particle force balance and particle trajectories of particles of mass m_p .

$$m_p \frac{d\overrightarrow{u_p}}{dt} = \sum_{i} \overline{F_i}$$
 (3)

$$\sum \overline{F_i} = \overline{F_D} + \overline{F_B} + \overline{F_G}$$
 (4)

$$m_p \frac{d\overrightarrow{u_p}}{dt} = m_p \frac{\overrightarrow{u} - \overrightarrow{u}_p}{\tau_r} + m_p \frac{\overrightarrow{u}(\rho_p - \rho)}{\rho_p} + \overrightarrow{F}$$
 (5)

The particles were assumed to be smooth and spherical. Stokes Cunningham drag law was used with default values of the coefficients for all particles which are given by equations 6, 7, and 8.

$$\overline{F_D} = \frac{3}{4} \frac{\rho}{\rho_p} \frac{d_p}{m_p} C_D(\vec{u} - \vec{u}_p) |\vec{u} - \vec{u}_p| \tag{6}$$

$$F_D = \frac{18\mu}{d_p^2 \rho C_C} \tag{7}$$

$$C_C = 1 + \frac{2\lambda}{d_p} (1.257 + 0.4) \tag{8}$$

The particle relaxation time was used for predicting particle trajectories using the force balance on the particle in the Lagrangian time frame as given in equation (5). This describes the deacceleration of particles due to the drag force and was solved using equation (9).

$$\tau_r = \frac{\rho_p d_p^2}{18\mu} \frac{24}{C_d Re} \tag{9}$$

Here Re is the relative Reynolds number and is calculated by:

$$Re_{p} = \frac{\left| \overrightarrow{u} - \overrightarrow{u_{p}} \right| \rho d_{p}}{\mu} \tag{10}$$

As the particles considered in this study are of small diameter, the torque or particle rotation was not considered. For sub-micron particles, it has been concluded from the literature that their dispersion is dominated by Brownian Force which is calculated using equation (11). The particle lifts for particle diameters greater than 1 µm can be solved using equation (12).

$$F_{bi} = \zeta_i \sqrt{\frac{216\rho v \sigma T}{\pi \rho_p^2 d_p^5 C_c \Delta t}}$$
 (11)

$$\vec{F} = m_p \frac{2Kv^{\frac{1}{2}}\rho d_{ij}}{\rho_p d_p (d_{lk}d_{kl})^{\frac{1}{4}}} (\vec{u} - \vec{u}_p)$$
(12)

The Discrete Random Walk Model or eddy lifetime model can be used to model particle interaction with discrete fluid phase turbulent eddies which are classified by random velocity fluctuations given by u', v', w' and are calculated as given below in equations (13)-(15), where ζ is a normally distributed random number. The value of the RMS (Root Mean Square) fluctuating components on the right-hand side of these equations is calculated by equation (16) using known values of kinetic energy turbulence at each point in the flow.

$$u' = \zeta \sqrt{u'^2} \tag{13}$$

$$v' = \zeta \sqrt{v'^2} \tag{14}$$

$$w' = \zeta \sqrt{w'^2} \tag{15}$$

The characteristic lifetime of an eddy is given by equation (16). The same can be calculated using equation (17) as random variation about T_L (calculated using equation 18), fluid Lagrangian integral time. Here, r is a uniform random number greater than zero and less than 1 and C_L is the integral time scale constant and.

$$\tau_e = 2T_L \tag{16}$$

$$\tau_e = -T_L \ln (r) \tag{17}$$

$$T_L = C_L \frac{k}{\epsilon} \tag{18}$$

For particle diameter generation, an exponential relation for particle diameter distribution of random nature using Rosin-Rammler relation was used. In this relation, the complete range of sizes is divided into an adequate number of discrete intervals; each represented by a mean diameter for which trajectory calculations are performed. If the size distribution is of the Rosin-Rammler type, the mass fraction of particles of diameter greater than d can be calculated using equation 19 where $\overline{\boldsymbol{d}}$ is the size constant and \boldsymbol{n} is the size distribution parameter. For the present study, a particle diameter range of 10μ m to 0.01μ m was used with a mean diameter of 0.5μ m.

$$Y_d = e^{-(d/\bar{d})^n} \tag{19}$$

METHODOLOGY

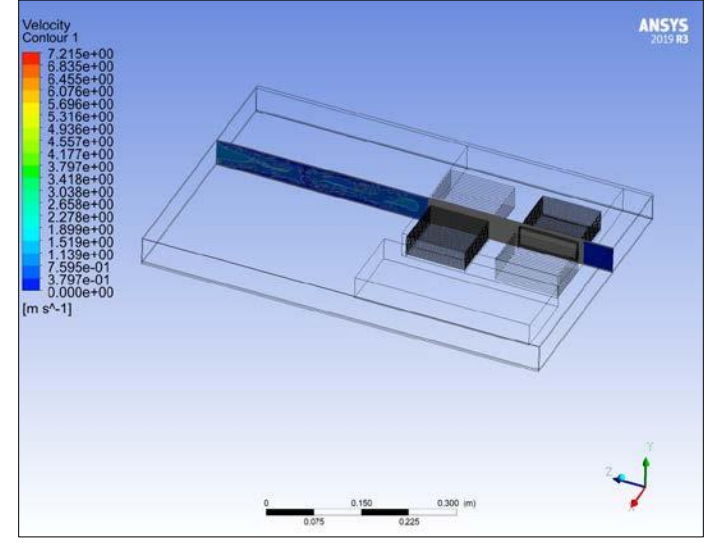
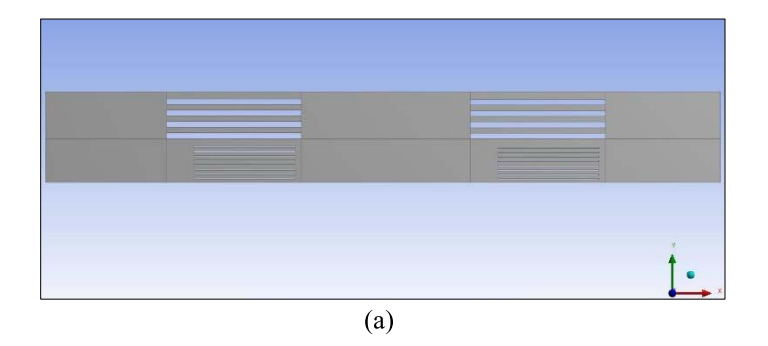


FIGURE 2: MODEL VOLUME AND VELOCITY DISTRIBUTION FOR A 3-D DESIGN OF A SERVER CHASSIS

To generalize the CFD results of particle dispersion, a set of assumptions was formulated that would most closely match flow parameters and conditions in a typical air-cooled data center. The range of particle diameter considered in this study is between 10um-0.01um with a mean diameter of 5um. A total of 15 different diameters were generated between this range to judge the dispersion of well-distributed particle sizes in the flow domain. The study initially began with 3-D models of servers of 1U and 2U form factor as shown in Figure 3, with detailed design of heat sinks, power distribution unit, and DIMMs modeled as blocks. After extracting the fluid volume, a refined mesh was generated with approximately 45 million elements. This led to high computation time because of which the modeling was done only in 2-D as sown in Figure 3. Various cases that have been simulated are tabulated in Table 3. These cases were simulated with two-particle densities and two different flow velocities. The particle densities chosen were 1550 kg/m³ and 4000 kg/m³, and the velocities were chosen to be 0.8 m/sec and 2.5 m/sec. The densities and were chosen based on data from literature of most pervasive and corrosive ionic salts and particulate matter. For velocities, the literature on airflow in data centers was referred. These cases were simulated both with and without the effect of gravitational force. The gravitation component was activated for simulations of blade servers and the case where the flow domain is visualized from the side to judge the impact of streamwise obstructions. The same was not activated while judging the impact of obstruction shapes, as would be seen if a server is viewed from the top when its cover is open. The flow domains were designed in ANSYS DM and the dimensions and design of the servers were inspired by widely used open compute servers in the industry.

S.No.	Case Type
1	2 Heat Sinks inline
2	2 heat sinks side by side
3	Heat sink with round edge
4	Heat Sink with sharp edges
5	Blade server
6	Staggered Heat sink arrangement
7	Heat sink with cutout

TABLE 3: DESCRIPTION OF SIMULATED CASES



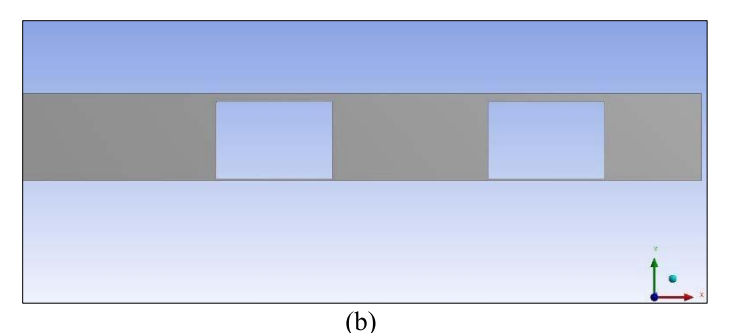


FIGURE 3: EXAMPLES OF THE SIMPLIFIED 2-D GEOMETRIES OF SERVERS USED FOR SIMULATIONS SHOWING (a) HEAT SINK AND DIMMS (b) HEAT SINKS IN LINE FROM SIDE VIEW

To reduce the simulation time while ensuring good results, the symmetric geometries were modeled with a symmetry boundary condition which also reduced the mesh count significantly. To ensure fast and reliable CFD simulation results, a fine quality mesh is paramount. For all the cases designed in the present study, consistent meshing operations were used in all the server designs. As turbulent flows in ducts are dominated by boundary layer effects, especially flows with bluff bodies and large obstructions, the mesh needs to be sufficiently dense near the walls. This is decided by the distance of the first cell from the wall based on the y⁺ value in the flow, where the y⁺ value is calculated using parameters like flow Reynolds number, hydraulic diameter, etc. For the present case, the y⁺ was kept below 3 by adding 10 inflation layers within a total thickness of 1 mm from the walls as shown in Figure 4. Mesh metrics like total skewness and mesh orthogonality were used to determine the mesh quality. For the CFD code used, a good mesh should have a skewness value closer to zero and orthogonality of less than 1. A uniform all quads structured grid was obtained for most of the cases with an average skewness of 0.08 and an orthogonality value of 0.9. The cases with multiple geometries were sliced to form sweepable faces for a structured grid. The maximum mesh count among all the cases was 439,000 which is significantly lower than that obtained in the 3-D model case.

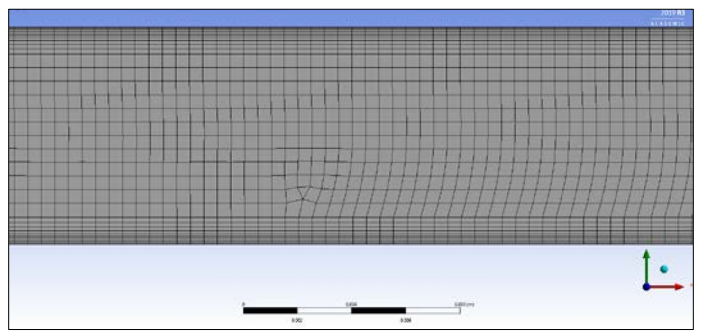


FIGURE 4: INFLATION LAYERS CREATED AT THE WALLS TO CAPTURE NEAR WALL VELOCITY GRADIENTS AND PARTICLE CONCENTRATIONS

For the current study, the effect of temperature and humidity were neglected as the main objective was to analyze and report particle dispersion and predict the most vulnerable locations of

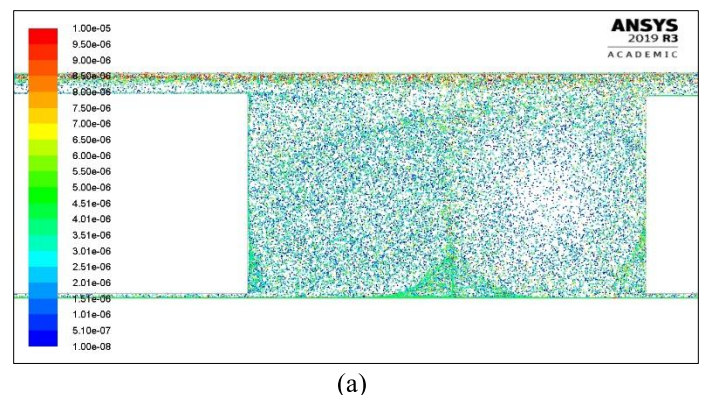
particle deposition. A transient analysis was done where a total simulation time of 5 seconds was used to fill the entire flow domain with enough particles to track. The particles were injected as surface injections at the inlet where particles were then released from each facet of the surface. Here, the facet value of a variable is defined as the computed arithmetic average of the adjacent cell values of the variable. The maximum, minimum, and mean diameters of the injections were specified. A constant mass flow rate was chosen 1e-16 kg/sec was chosen and for size distribution. The initial velocity of particles was also chosen to be the same as for the flow velocity. For particle specific flow models, two-way coupling was used in which the continuous flow field was solved first, after which the discrete phase trajectories are calculated. After this, the continuous phase was solved again based on interphase momentum exchange (as no heat and mass transfer is considered in this study) and discrete phase trajectories were then recalculated for a modified flow field. This process was repeated until a converged solution was obtained. For the current study, a DPM iteration interval of 10 was selected, which means that a discrete phase iteration was performed every tenth continuous phase iteration. A time step size of 0.01 seconds was chosen with a total number of iterations equal to 500 and maximum iterations per time step equal to 20 to achieve convergence for each time step.

RESULTS AND DISCUSSION

A total of 16 simulation cases were solved for different categories of server geometries and flow conditions based on varying particle density and velocity. To judge the probability of particle deposition, the elapsed residence time of particles within the flow domain, and total particle mass escaping the outlet was analyzed. As mentioned earlier, a mass flow rate of 1e-16 kg/sec was injected in the flow domain, meaning that a total particle mass of 5e-16 kg passed through the domain. The results are broadly divided into 5 different case categories as presented in the coming sections and repetitiveness of results was avoided by consolidating the particle summary in tables. The drag coefficient monitor was used to determine if the flow has reached steady-state or not. This was done as absolute convergence or monitoring of residuals is not necessarily an indicator of converged solution for highly turbulent flows with bluff bodies. The effect of gravity was neglected for some cases as the flow inside the servers is only dominated by forced convection.

5.1 Sharp-edged heat sink v/s curved edge

A lot of heat sinks are manufactured with curved edges, especially for servers requiring very high airflow rates, to reduce the overall pressure drop in the system. This decelerates the flow at the corners, keeping the turbulent mixing between the fins for effective heat removal. In this case, 2-D geometries were designed with the dimensions equivalent to that of a 2U server and a heat sink height of 7.8 cm.



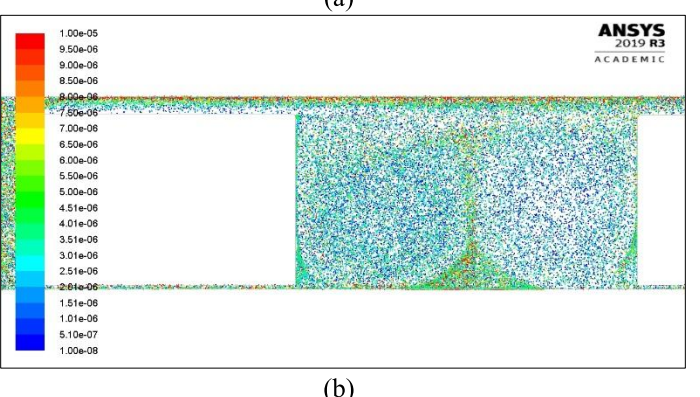


FIGURE 5: PARTICLE DIAMETERS IN THE FLOW DOMAIN FOR DISPERSION FROM (a) SHARP AND (b) ROUND EDGED HEAT SINKS

As seen in Figure 5 (a) and 5 (b), for sharp-edged heat sink more particle diameters were present on the heat sink in sharp edge than in the case of the round edge heat sink. Also, as opposed to that, more particle diameters were present between heat sinks in case round-cornered than sharp edge heat sink Furthermore, a greater number of the particles moved towards the top of the server for the round edge heat sink. A comparison of particle flow parameters is given in Table 5 and Table 6. It can be concluded that more particles stay in the flow domain for sharp-cornered heat sinks. This can be attributed to the fact that sharp edges tend to shed more vortices, trapping the particles of larger diameters in the around them due to the centrifugal forces. This has also been reported in the published literature.

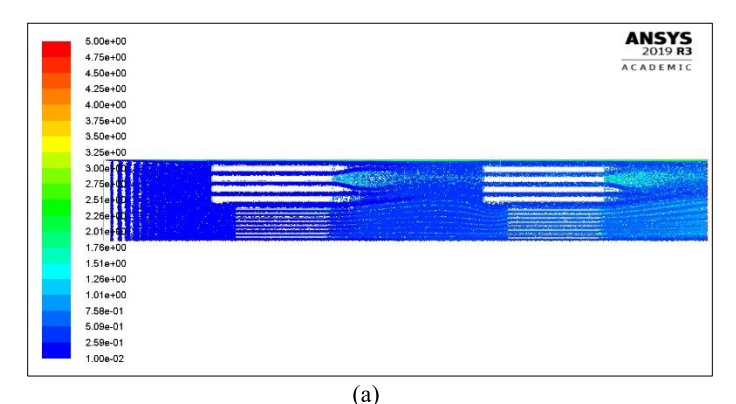
Parameter	Value
Total mass injected	5e-20 kg
Escaped Outlet	3.9e-16 kg
Max time in domain	2.36e-1 sec
Min time in the domain	4.93 sec

TABLE 4: PARTICLE SUMMARY FOR SHARP EDGE HEAT SINK

Parameter	Value
Total mass injected	5e-20 kg
Escaped Outlet	4.5e-20 kg
Min time in the domain	2.30e-01 sec
Max time in the domain	4.64 sec

TABLE 5: PARTICLE SUMMARY FOR ROUND EDGE HEAT SINK

5.2 Heat sinks side by side v/s in line



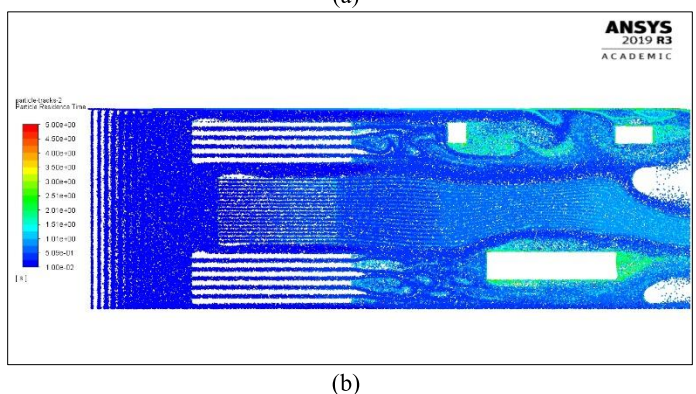


FIGURE 6: PARTICLE RESIDENCE TIME IN THE FLOW DOMAIN FOR (a) IN-LINE HEAT SINKS (b) SIDE BY SIDE HEAT SINKS

As mentioned earlier in this study, it is imperative to generalize the results obtained from these simulations for the most common server geometries. The geometries shown in Figure 6 were decided based on a general survey by the authors for storage products offered by leading server manufacturers. Symmetry boundary condition was used for bottom walls in both cases. Additional obstructions were added to observe the effect of varying geometrical shapes within the server. These geometrical features also represent other components within the server like power distribution trays inside the chassis, smaller heat sinks for chipsets, etc. As seen in the figure above, high particle residence time was obtained at the walls of in-line heat sinks towards the rear end of the server. Other locations of relatively higher residence time were between the heat sink and the DIMMs. Another inference that can be made from Figure 6 (b) is that solid obtructions behind the heat sinks with greater depth do not create large turbulent eddies or any vortex shedding when compared to square or circular obstructions. It can thus be pointed out that there might be a greater probability of finding settled particulate matter towards the rear end of the servers of similar geometries. These regions mostly contain drive backplanes, power supplies, drive fillers, etc. Table 6 and Table 7 show the comparison particle summary for both the cases discussed in this section. Here, it can be noted that for both the cases, the maximum time spent by the particles in the flow domain was identical, but the average time was more in case of heat sinks located side by side.

Parameter	Value
Total mass injected	5e-16 kg
Escaped Outlet	4.3e-16 kg
Min time in the domain	3.9e-01 sec
Max time in the domain	4.9 sec

TABLE 6: PARTICLE SUMMARY FOR IN-LINE HEAT SINKS HIGH DENSITY

Parameter	Value
Total mass injected	5e-16 kg
Escaped Outlet	4.2e-16 kg
Min time in the domain	4.1e-01 sec
Max time in the domain	4.9 sec

TABLE 7: PARTICLE SUMMARY FOR HEAT SINKS ARRANGED SIDE BY SIDE HIGH DENSITY

5.3 Blade Servers

As mentioned earlier, the effect of gravity can be neglected when considering the case of forced convection. This might not be completely true for the case of blade servers, where a chassis form factor of up to 8U is present in enclosures. In these cases, gravitational effects can have a significant impact on particle deposition within the enclosure. Table 8 and Table 9 show the impact of varying density within a blade server. It was observed that more particles are trapped for a longer period within the fins of the heat sinks as the effect of gravity is included as compared to the previous case for the inline case in Figure 6 (a).

Parameter	Value
Total mass injected	5e-16 kg
Escaped Outlet	4.3e-16 kg
Min time in the domain	3.8e-01 sec
Max time in the domain	4.6 sec

TABLE 8: PARTICLE TRANSFER SUMMARY FOR LOW-DENSITY PARTICLES IN A BLADE SERVER

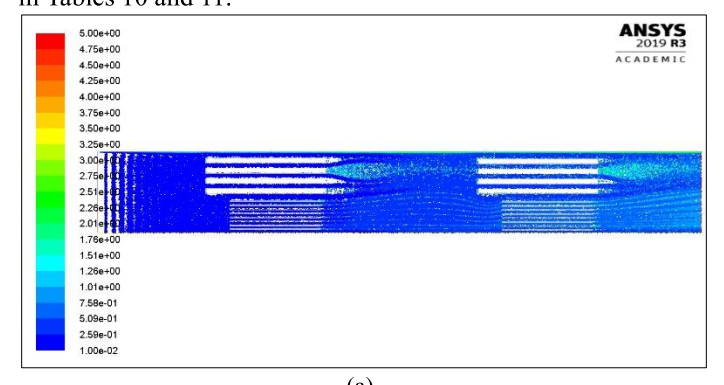
Parameter	Value
Total mass injected	5e-16 kg
Escaped Outlet	4.2e-16 kg
Min time in the domain	3.8e-01 sec
Max time in the domain	4.5 sec

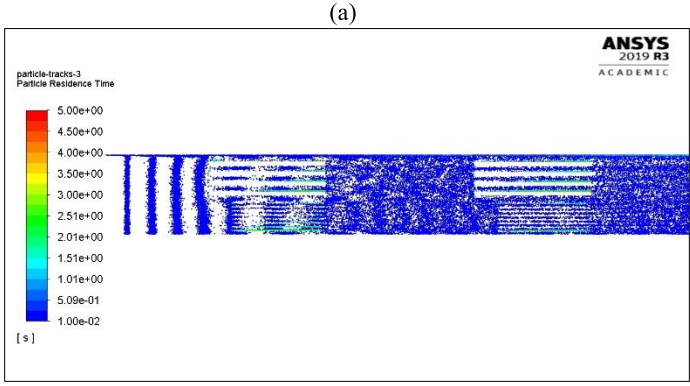
TABLE 9: PARTICLE TRANSFER SUMMARY FOR HIGH-DENSITY PARTICLES IN A BLADE SERVER

5.4 Effect of velocity

To assess the impact of increasing inlet velocity on particle accumulation, two different values of velocities were chosen from published literature [48]. The particle residence time plots

depict that for lower velocity value, particles spend more time in the flow domain and for high velocity, particles spend more time on the surfaces. This phenomenon holds when compared to the conclusions made by Frankenthal et al [45]. No deposition on top or bottom wall for high velocity was observed until the flow reaches the second set of DIMMs. The comparison of residence time and mass transfer through the outlet in both cases is shown in Tables 10 and 11.





(b)

FIGURE 7: PARTICLE RESIDENCE TIME IN THE FLOW

DOMAIN FOR IN-LINE HEAT SINKS (a) LOW VELOCITY (b)

HIGH VELOCITY

Parameter	Value
Total mass injected	5e-16 kg
Escaped Outlet	4.2e-16 kg
Min time in the domain	3.8e-01
Max time in the domain	4.5 sec

TABLE 10: PARTICLE TRANSFER SUMMARY FOR LOW-VELOCITY FLOW WITH HIGH-DENSITY PARTICLES

Parameter	Value
Total mass injected	5e-16 kg
Escaped Outlet	4.8e-16 kg
Min time in the domain	1.4e-01
Max time in the domain	4.6 sec

TABLE 11: PARTICLE TRANSFER SUMMARY FOR HIGH-VELOCITY FLOW WITH HIGH-DENSITY PARTICLES

5.5 Effect of the heat sink cutout

Cutouts can be provided on narrow as well as high form factor heat sinks to reduce pressure drops. To observe the effect of change of geometry within the heat sink, a heat sink cutout was provided at the center of the sink as shown in Figure 8. As it can

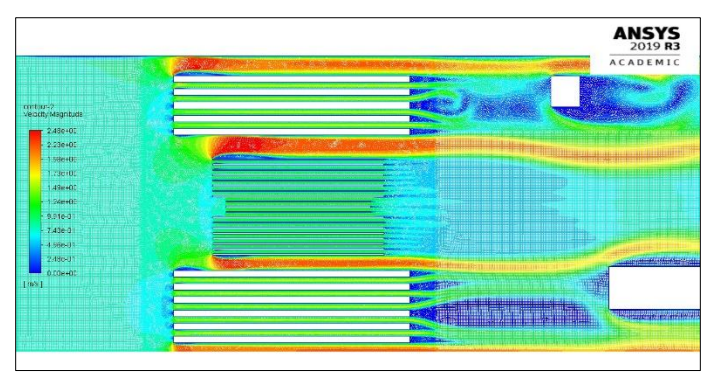


FIGURE 7: FLOW VELOCITY CONTOUR FOR HEAT SINK CUTOUT CASE

be seen in Table 12 and Table 13, the heat sink cutout caused a reduction in total mass escaping the outlet meaning more particles are trapped within the flow domain. Although the total reduction might seem a very small number, this can be significantly higher over hours of operation. This increase in particle count within the flow domain might be due to a reduction in total static pressure value around the fins which might cause a local deposition of particles in the surrounding region. This was also observed in particle residence time plots.

Parameter	Value
Total mass injected	5e-16 kg
Escaped Outlet	4.2e-16 kg
Min time in the domain	4.1e-01 sec
Max time in the domain	4.9 sec

TABLE 12: PARTICLE TRANSFER SUMMARY FOR HEAT SINK CUTOUT, LOW DENSITY

Parameter	Summary
Total mass injected	5e-16 kg
Escaped Outlet	4.4e-16 kg
Min time in the domain	4.1e-01 sec
Max time in the domain	4.98 sec

TABLE 13: PARTICLE SUMMARY FOR HEAT SINK WITHOUT CUTOUT, LOW DENSITY

CONCLUSION

Particle transport and dispersion within simplified data center storage systems were studied using CFD. Predictions for particle accumulation were made based on analysis of total elapsed time that the particles spend before escaping from the flow domain and by analyzing the difference of mass transferred between inlet and outlet of the flow domains. Based on the nature of flow obstructions present within the server, it was observed that while there might be little accumulation near thin features like DIMMS and heat sinks, the presence of other components and smaller features can significantly increase it. Also, for features with aspect ratios of any dimension closer to 1 may have

significant particle accumulation around it. On the contrary, features with larger length offer significantly less flow resistance and may be less vulnerable to deposition. Critical components, as per failure rates are concerned, are usually hard drives. Most of the storage servers today have separate hard drive bays. The servers where the hard drives are located towards the rear end might be more prone to exposure to particulates. It was also seen that higher velocities tend to increase accumulation on flat surfaces like fins and the DIMMs, therefore, for computational servers that are air-cooled, they might experience increased exposure to particles when the data center is operating in free air cooling mode. While novel cooling methods like phase-change, direct immersion cooling, and liquid cooling [49-52] are mostly being used for high-performance computing, most storage systems based data centers will continue to use air cooling. Therefore, it becomes imperative to address the challenge of particulate contamination for economizer based or free aircooled data centers.

FUTURE WORK

This study was a first step towards establishing a predictive approach to how the particles might behave after entering the data center equipment while economizer or free air-cooling mode is on. Based on conclusions drawn from this study, further investigations will be conducted at a larger scale where the spatial distribution of particles will be determined in a data center with multiple rows of racks. The simulations can be made complicated by varying pressure across each of these rows to represent a more realistic scenario. The effects of temperature and, therefore, thermophoresis force can be included by treating particles as volatile and reacting species as they move through the flow domain. A 2-D study is already being conducted by the authors to simulate the chemical reaction that occurs at the material level in presence of ionic species in the flow by varying the humidity and temperature of the flow domain.

ACKNOWLEDGMENT

This work is supported by NSF I/UCRC in Energy-Smart Electronic Systems (ES2). The authors would also like to extend special gratitude towards Mark Seymour and Kourosh Nemati of Future Facilities for their guidance and feedback throughout the project.

REFERENCES

- [1] Koomey, Jonathan. "Growth in data center electricity use 2005 to 2010." A report by Analytical Press, completed at the request of The New York Times 9 (2011): 161.
- [2] Prabjit Singh, Levente Klein, Dereje Agonafer, Jimil M. Shah and Kanan D. Pujara, "Effect of Relative Humidity, Temperature and Gaseous and Particulate Contaminations on ITE Reliability, DOI: 10.1115/IPACK2015-48176, ASME InterPACK 2015, San Francisco, CA.

- [3] Shah, Jimil & Awe, Oluwaseun & Gebrehiwot, Betsegaw & Agonafer, Dereje & Singh, P & Kannan Mestex, Naveen & Kaler Mestex, Mike. (2017). "Qualitative Study of Cumulative Corrosion Damage of ITE in a Data Center Utilizing Air-side Economizer Operating in Recommended and Expanded ASHRAE Envelope". Journal of Electronic Packaging. 139. 021002. 10.1115/1.4036363.
- [4] Thermal Guidelines for Data Processing Environments, ASHRAE Datacom Series, 1st Edition, 2004, ASHRAE, Atlanta, GA USA
- [5] Thermal Guidelines for Data Processing Environments, ASHRAE Datacom Series, 2nd Edition, 2008, ASHRAE, Atlanta, GA, USA.
- [6] Thermal Guidelines for Data Processing Environments, ASHRAE Datacom Series, 3rd Edition, 2012, ASHRAE, Atlanta, GA, USA
- [7] https://www.opencompute.org/blog/cooling-an-ocp-data-center-in-a-hot-and-humid-climate
- [8] Google. Efficiency: How We Do It, 2014
- [9] Microsoft Microsoft Shares Video Tour of its Cloud Datacenters, 2011
- [10] Burnett W. H., F. S. Sandroff and S. M. D'Egidio, "Circuit failure due to fine dust mode particulate air pollution," ISTFA '92, The 18th Int'l Symposium for Testing & Failure Analysis, Los Angeles, CA, 17-23 Oct 1992, 329-333.
- [11] Cole, M., L. Hedlund. T; Kiraly, S. Nickel, P. Singh and T. Tofil, "Harsh Environmental Impact on Resistor Reliability", SMTA Int'l Conf, Proc., 24 Oct 2010.
- [12] Directive 2002/95/EC of the European Parliament and of the Council of 27 January 2003 on the Restriction of the use of Certain Hazardous Substances on Electrical and Electronic Equipment Official Journal L 037, February 13, 2003, 19-23.
- [13] Fu, H., C. Chen, P. Singh, J. Zhang. A. Kurella, X. Chen, X. Jiang, J. Burlingame and S. Lee, "Investigation of Factors that Influence Creep Corrosion on Printed Circuit Boards," SMTA Pan Pacific Microelectronics Symposium, Kauai, 14-16 Feb 2012.
- [14] Fu, H., C. Chen, P. Singh, J. Zhang. A. Kurella, X. Chen, X. Jiang, J. Burlingame and S. Lee, "Investigation of Factors that Influence Creep Corrosion on Printed Circuit Boards, Part 2", SMTAI 2012.
- [15] ASHRAE Technical Committee 9.9. 2009. "2009 Particulate and Gaseous Contamination Guidelines for Data Centers."
- [16] Muller, Chris. (2014). "Reliability Concerns for Data Center ITE: Contamination Issues, Standards Actions, and Case Studies".
- [17] ASHRAE. 2013. "Particulate and Gaseous Contamination in Datacom Environments", 2nd Ed. Atlanta: American Society of Heating, Refrigerating, and Air-Conditioning Engineers, Inc. [18] ISA. 2013. ANSI/ISA 71.04-2013: Environmental Conditions for Process Measurement and Control Systems: Airborne Contaminants. Research Triangle Park: International Society for Automation.

- [19] iNEMI. 2012. iNEMI Position Statement on the Limits of Temperature, Humidity and Gaseous Contamination in Data Centers and Telecommunication Rooms to Avoid Creep Corrosion on Printed Circuit Boards.
- [20] China National Standard GB 50174-2008: Code for Design of Electronic Information System.
- [21] Satyam Saini, Pardeep Shahi, Pratik Bansode, Ashwin Siddarth, Dereje Agonafer "CFD Investigation of Dispersion of Airborne Particulate Contaminants in a Raised Floor Data Center", SEMI-THERM 36, March 16-20, 2020
- [22] Jimil M. Shah, Roshan Anand, Satyam Saini, Rawhan Cyriac, Dereje Agonafer, Prabjit Singh, Mike Kaler, 2019, Development of A Technique to Measure Deliquescent Relative Humidity of Particulate Contaminants and Determination of the Operating Relative Humidity of a Data Center, ASME Conference Paper No. IPACK2019-6601
- [23] Gautham Thirunavakkarasu, Satyam Saini, Jimil Shah, Dereje Agonafer,2018, Airflow pattern and path flow simulation of airborne particulate contaminants in a high-density Data Center utilizing Airside Economization, ASME Conference Paper No. IPACK2018-8436
- [24] Seymour, M.J., A. A. M. A., and Jiang, J., 2000. "Cfd based airflow modelling to investigate the effectiveness of control methods intended to prevent the transmission of airborne organisms". Air Distribution in Rooms, (ROOMVENT 2000).
- [25] Jones, P., and Whittle, G., 1992. "Computational fluid dynamics for building air flow prediction- current status and capabilities". Building and Environment, 27(3), pp. 321–338.
- [26] Chen, Q., and Zhang, Z., 2005. "Prediction of particle transport in enclosed environment". China Particuology, 3(6), pp. 364–372.
- [27]. Longmire, E. K., and Eaton, J. K. (1992). Structure of a Particle-Laden Round Jet, *J. Fluid Mech.* 236:217–257.
- [28] Lazaro, B. J., and Lasheras, J. C. (1992). Particle Dispersion in the Developing Free Shear Layer, Part 1—Unforced Flow, *J. Fluid Mech.* 235:143–178.
- [29]. Crowe, C. T., Chung, J. N., and Trout, T. R. (1988). Particle Mixing in Free Shear Flows, *Progress in Energy and Combustion Science* 14:171–194.
- [30] Uthuppan, J., Aggarwal, S. K., Grinstein, F. F., and Kailasanath, K. (1994). Particle Dispersion in a Transitional Axisymmetric Jet: A Numerical Simulation, *AIAA J.* 32:2004–2014.
- [31] Aggarwal, S. K. (1994). Relationship Between the Stokes Number and Intrinsic Frequencies in Particle-Laden Flows, *AIAA J.* 32:1322–1325.
- [32] Chang, E., and Kailasanath, K. (1996). Simulation of Dynamics in a Confined Shear Flow, AIAA J. 34:1160–1166
- [33] D. J. Brandon & S. K. Aggarwal (2001) A Numerical Investigation of Particle Deposition on a Square Cylinder Placed in a Channel Flow, Aerosol Science & Technology, 34:4, 340-352
- [34] Alletto, M., & Breuer, M. (2012). One-way, two-way and four-way coupled LES predictions of a particle-laden turbulent flow at high mass loading downstream of a confined bluff body. *International Journal of Multiphase Flow*, 45, 70–90.

- [35] van Vliet, E., Singh, M., Schoonenberg, W., van Oord, J., van der Plas, D., & Deen, N. (2013). *Development and validation of Lagrangian-Eulerian multi-phase model for simulating the argon stirred steel flow in a ladle with slag.* Proceedings of the 5th International Conference on Modelling and Simulation of Metallurgical Processes in Steelmaking, STEELSIM. Ostrava, Czech Republic.
- [36] Sardina, G., Schlatter, P., Brandt, L. P., & Casciola, C. (2012). Wall accumulation and spatial localization in particle-laden wall flows. *Journal of Fluid Mechanics*, 699, 50–78.
- [37] Wang, B., Manhart, M., & Zhang, H. (2011). Analysis of inertial particle drift dispersion by direct numerical simulation of two-phase wall-bounded turbulent flows. *Engineering Applications of Computational Fluid Mechanics*, 5(3), 341–348. [38] Vreman, A. (2015). Turbulence attenuation in particle-laden flow in smooth and rough channels. *Journal of Fluid Mechanics*, 773, 103–136
- [39] Franziska Greifzu, Christoph Kratzsch, Thomas Forgber, Friederike Lindner & Rüdiger Schwarze (2016) Assessment of particle-tracking models for dispersed particle-laden flows implemented in OpenFOAM and ANSYS FLUENT, Engineering Applications of Computational Fluid Mechanics, 10:1, 30-43, DOI: 10.1080/19942060.2015.1104266 [40]LBNL report
- [41] Pui DYH, Romay-Novas F, Liu BYH. Experimental study of particle deposition in bends of circular cross-section. Aerosol Sci Technol 1997;7:301–15
- [42] Zhang H, Ahmadi G. Aerosol particle transport and deposition in vertical and horizontal turbulent duct flows. J Fluid Mech 2000;406:55–80.
- [43] Zhao Bin, Wu Jun. Modeling particle fate in ventilation system—Part II: Case study. Build Environ 2009;44:612–20.
- [44] Gao, R., and Li, A. (2012). Dust Deposition in Ventilation and Air-Conditioning Duct Bend Flows. *Energy Convers. Manage.*, 55:49–59
- [45] Frankenthal
- [46] ANSYS® ANSYS FLUENT Theory Guide, Chapter 16, Release 2019 R3
- [47] ANSYS® ANSYS FLUENT User's Guide, Chapter24, Release 2019 R3
- [48] Ibrahim, Mahmoud, et al. "Thermal mass characterization of a server at different fan speeds." *13th InterSociety Conference on Thermal and Thermomechanical Phenomena in Electronic Systems*. IEEE, 2012.
- [49] Shah, J. M., Eiland, R., Rajmane, P., Siddarth, A., Agonafer, D., and Mulay, V. (April 10, 2019). "Reliability Considerations for Oil Immersion-Cooled Data Centers." ASME. J. Electron. Packag. June 2019; 141(2): 021007. https://doi.org/10.1115/1.4042979
- [50]Ramdas, Shrinath, Rajmane, Pavan, Chauhan, Tushar, Misrak, Abel, and Agonafer, Dereje. "Impact of Immersion Cooling on Thermo-Mechanical Properties of PCB's and Reliability of Electronic Packages." Proceedings of the ASME 2019 International Technical Conference and Exhibition on Packaging and Integration of Electronic and Photonic Microsystems. ASME 2019 International Technical Conference

- and Exhibition on Packaging and Integration of Electronic and Photonic Microsystems. Anaheim, California, USA. October 7–9,2019.V001T02A011.ASME.https://doi.org/10.1115/IPACK2019-6568
- [51] Shahi, Pardeep, 2016, "Experimental Analysis of PCM based Thermal Storage System for Solar Power Plant," M.S. thesis, Indian Institute of Technology- Mumbai.
- [52] Kumar, Ashish, Pardeep Shahi, and Sandip K. Saha. "Experimental Study of Latent Heat Thermal Energy Storage System for Medium Temperature Solar Applications."
- [53] Dehkordi, B. G., Fallah, S., & Niazmand, A. (2014). Investigation of harmonic instability of laminar fluid flow past 2D rectangular cross sections with 0.5–4 aspect ratios. *Proceedings of the Institution of Mechanical Engineers, Part C: Journal of Mechanical Engineering Science*, 228(5), 828–839. https://doi.org/10.1177/0954406213491906